Appl Phys B (2011) 104:1019–1027
DOI 10.1007/s00340-011-4589-x

Applied Physics B
Lasers and Optics

Photoluminescence, thermoluminescence and electron spin resonance studies on Eu^{3+} doped $Ca_3Al_2O_6$ red phosphors

V. Singh · S. Watanabe · T.K. Gundu Rao · I.-J. Lee

Received: 14 December 2010 / Revised version: 14 April 2011 / Published online: 4 June 2011

Abstract Tricalcium aluminate doped with Eu^{3+} was prepared at furnace temperatures as low as 500°C by using the convenient combustion route and examined using powder X-ray diffraction, scanning electron microscope and photoluminescence techniques. A room-temperature photoluminescence study showed that the phosphors can be efficiently excited by UV/Visible region, emitting a red light with a peak wavelength of 616 nm corresponding to the $^5D_0$–$^7F_2$ transition of Eu^{3+} ions. The phosphor exhibits three thermoluminescence (TL) peaks at 195°C, 325°C and 390°C. Electron Spin Resonance (ESR) studies were carried out to study the defect centres induced in the phosphor by gamma irradiation and also to identify the defect centres responsible for the TL process. Room-temperature ESR spectrum of irradiated phosphor appears to be a superposition of three distinct centres. One of the centres (centre I) with principal g-value 2.0130 is identified as O^- ion while centre II with an axially symmetric principal values $g_\parallel = 2.0030$ and $g_\perp = 2.0072$ is assigned to an F^+ centre (singly ionized oxygen vacancy). O^- ion (hole centre) correlates with the TL peak at 195°C and the F^+ centre (electron centre), which acts as a recombination centre, is also correlated to the 195°C TL peak. F^+ centre further appears to be related to the high temperature peak at 390°C. Centre III is also assigned to an F^+ centre and seems to be the recombination centre for the TL peak at 325°C.

V. Singh (✉)
Department of Chemistry, Kyungpook National University,
Daegu 702701, Republic of Korea
e-mail: vijayjiin2006@yahoo.com

S. Watanabe · T.K. Gundu Rao
Institute of Physics, University of Sao Paulo, 05508-090
Sao Paulo, SP, Brazil

I.-J. Lee (✉)
Department of Chemistry, Dongguk University,
707 Suckjang-dong, Gyeongju-Si, Gyeongbuk 780-714, Korea
e-mail: lii@dongguk.ac.kr

1 Introduction

Alkaline earth aluminate phosphors doped with rare-earth ions are of great importance in the field of optical and light emission applications [1–5]. In the past decade, synthesis and physical characterization of rare-earth doped calcium aluminates have generated significant interest and are still being investigated, owing to their importance as luminescent host for the next generation of displays and lighting devices [6–10]. In recent years, significant efforts have been made by several research groups towards the synthesis and characterization of rare-earth as well as transition metal ions doped calcium aluminate phosphors [6–13]. There are reports on the calcium aluminates which indicate that they are important ceramic materials for high temperature refractory applications [14–16]. Goktas and Weinberg [17] indicated that some amorphous calcium aluminate compositions are photosensitive and therefore potential candidates for optical information storage devices. Tricalcium aluminate ($Ca_3Al_2O_6$) is one of the main phases in the cement chemistry. We note here that the several research articles on the crystallographic studies and synthesis have been published on $Ca_3Al_2O_6$ (C_3A) [18–21]. In the literature, there are only few reports on the synthesis of C_3A by low temperature methods and also C_3A has not been received much attention as luminescent host. Hence in the present work, we have successfully employed a low temperature, fast, simple and safe combustion process for the preparation of Eu^{3+} doped $Ca_3Al_2O_6$ material.

Eu^{3+} doped inorganic phosphors have been widely investigated due to their potential applications in solid state illumination as red emitting phosphors for improving the rendering index. The phosphor coating in devices is continuously hit by ionizing radiations in order to convert to visible light output. In such a situation, the formation of defect centres can be expected. These radiation-induced defects can play a significant role in influencing the thermal, electrical, optical and magnetic properties of the solids [22, 23]. In this respect, a study of radiation defects and a complete knowledge about the type of defects is of a great practical importance in order to evaluate an irradiation performance of phosphor materials and to develop innovative materials with superior properties. There are several reports on newly developed phosphor materials but understanding of radiation-induced defects and their behaviour is still lacking. Thermoluminescence (TL) is one of the techniques available for the investigation of defects in solid materials. Another sensitive technique used in the investigation of defects is electron spin resonance (ESR). During the past decade, studies on rare-earth as well as actinide doped phosphates, borates, sulphates, sulfides and aluminates have shown that the defect centres are intimately related to the process of TL in these phosphors [24–29]. The release of hole/electron from defect centres at the characteristic trap site initiates the luminescence process in these materials. These aspects have been clearly demonstrated in the above mentioned phosphors using TL and ESR techniques. In recent years, we have investigated the radiation-induced defect centres due to external gamma irradiation in a variety of inorganic phosphors doped with rare earth using TL and ESR techniques [28–32].

In the present work, combustion synthesized powder samples were characterized by X-ray diffraction (XRD), scanning electron microscopy (SEM) and photoluminescence (PL). Europium was incorporated as Eu^{3+} in $Ca_3Al_2O_6$ phosphor. In addition, we have studied the correlation between the TL peaks and the centres monitored via its ESR spectrum.

2 Experimental

2.1 Sample preparation

Pure and Eu doped $Ca_3Al_2O_6$ samples were synthesized by combustion method with $Ca(NO_3)_2{\cdot}4H_2O$, $Al(NO_3)_3{\cdot}9H_2O$, $Eu(NO_3)_3{\cdot}5H_2O$ and CH_4N_2O as starting materials. Urea (CH_4N_2O) was added as a fuel for combustion and its amount was calculated using total oxidizing (O) and reducing valences (F) based on the concept of propellant chemistry, as reported earlier [33–39]. Nominal amount of the starting materials were weighed and mixed in an agate mortar to obtain a final product of the chemical formula $Ca_3Al_2O_6{:}Eu_{0.07}$. The mixing resulted in a thick paste due to large crystallization of water in aluminium nitrate. The resulting paste was transferred into a china dish and the dish was introduced into a muffle furnace maintained at 500°C. Initially, the paste melts and undergoes dehydration followed by decomposition with the evolution of large amounts of gases (oxides of nitrogen and ammonia). The mixture then froths and swells forming a foam, which ruptures with a flame and glows to incandescence. The entire combustion process is over in less than 5 min. The foam is then crushed into powder and is used for further characterization.

2.2 Instruments

Powder XRD experiments were performed on a Philips X′ pert X-ray diffractometer with graphite monochromatized CuK_α radiation ($\lambda = 0.15418$ nm) in the 2θ range from 10° to 70°. Photoluminescence spectra in the spectral range 220–750 nm were recorded at room temperature on a Hitachi F-4500 FL Spectrophotometer with spectral slit widths of 1.5 nm. Scanning electron micrographs (SEM) were taken on a Hitachi S-4300 scanning electron microcope. A ^{60}Co gamma source was used for the irradiation of samples. TL experiments were carried out on a Daybreak 1100 series automated TL reader system with a heating rate of 5°C/sec in a nitrogen atmosphere. Electron spin resonance experiments were carried out on a Bruker EMX ESR spectrometer operating at X-band frequency with 100 kHz modulation frequency. Diphenyl Picryl Hydrazyl (DPPH) was used for calibration of g-values of defect centres. The temperature dependence of the ESR spectra was studied using Bruker B VT 2000 variable temperature accessory.

3 Results and discussion

3.1 X-ray diffraction

The formation of the compound was confirmed by XRD. The XRD pattern of as-prepared host ($Ca_3Al_2O_6$) without any doping is shown in Fig. 1. All the major reflections in Fig. 1 could be indexed to the standard cubic $Ca_3Al_2O_6$ (JCPDS, 32-0149). It has been reported in the literature that phase-pure $Ca_3Al_2O_6$ does not exist at lower temperature synthesis process and even after sintering at 1400°C, weak reflections of CaO and $Ca_{12}Al_{14}O_{33}$ phases were identified. Williamson and Glasser [40] reported $Ca_{12}Al_{14}O_{33}$ to be the principal non-equilibrium phase, although $CaAl_2O_4$ was also observed. In a later publication, Singh et al. [41] also mentioned the presence of several aluminate phases such as $CaAl_4O_7$, $CaAl_2O_4$ and $Ca_{12}Al_{14}O_{33}$.

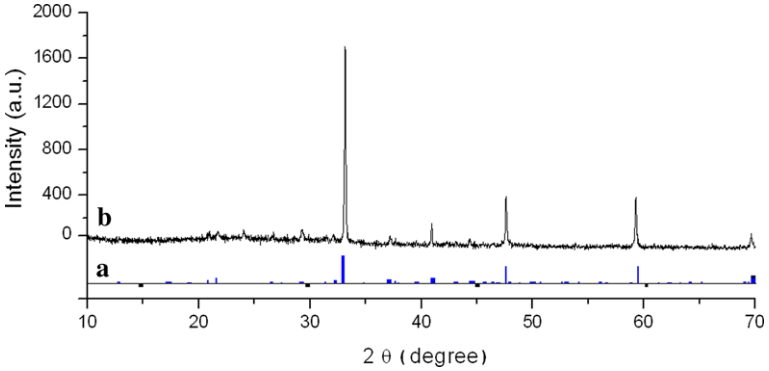

Fig. 1 Powder XRD patterns of *a* reference $Ca_3Al_2O_6$, JCPDS No. 32-0149 and *b* as-prepared $Ca_3Al_2O_6$ powder

3.2 Scanning electron microscopy

The representative SEM micrographs for the host ($Ca_3Al_2O_6$) without any doping are shown in Fig. 2. It can be clearly observed from low resolution and large covered area SEM (Fig. 2A) that powders are in the form of agglomerates with non-uniform shapes and sizes. In addition, there are some plates containing pores while the pores are also absent in some plates. This non-uniformity in shapes, sizes and porosity is caused by the (i) non-uniform distribution of temperature and (ii) irregular mass flow during combustion. The high resolution SEM of the foam contains a number of pores formed by the escaping gases during combustion and can be seen in Fig. 2B (magnified view of Fig. 2A (zone a)) and Fig. 2C (magnified view of Fig. 2B (zone b)). The foamy microstructure of the aluminates reflects inherent nature of the combustion process.

3.3 Photoluminescence

Figures 3(a) and (b) show photographs of the as-prepared $Ca_3Al_2O_6$:Eu^{3+} powders under room light and 254 nm UV irradiation, respectively. Under 254 nm excitation source, the white powder gives red colour, with no dark patches. Figure 4 shows the photoluminescence spectra of as-prepared $Ca_3Al_2O_6$:Eu^{3+} (a) excitation spectrum (λ_{em} = 616 nm) and (b) emission spectrum ($\lambda_{ex} = 255$ nm) at room temperature. The excitation spectrum contains an intense broad band with a maximum at 255 nm arising from the charge transfer band (CTB) between Eu^{3+} and the neighbouring O^{2-} and a group of lines in the longer wavelength region due to the f–f transitions within $Eu^{3+}4f^6$ configuration. The lines around 396 nm ($^7F_0 \rightarrow {}^5L_6$) and 466 nm ($^7F_0 \rightarrow {}^5D_2$) are the most noticeable. It can be seen clearly that the intra-configuration $4f^6$ excitation lines (396 nm, 466 nm) are very weaker than the charge transfer transition from the O^{2-} to Eu^{3+}. The emission spectrum was monitored with the intense charge transfer band at 255 nm. It should be noted here that the position of the CTB band at 255 nm is suitable for Hg discharge-based lamp applications. Under 255 nm excitation, the emission spectrum of $Ca_3Al_2O_6$:Eu^{3+} phosphor is composed of several sharp lines, which belong to the characteristic emission of trivalent Eu ion. The emission spectrum is dominated by the main lines at 616 nm due to the $^5D_0$–$^7F_2$ transition and 594 nm due to the $^5D_0$–$^7F_1$ transition. The peaks from $^5D_0$–$^7F_2$ (electric-dipole transition) is stronger than that from $^5D_0$–$^7F_1$ (magnetic-dipole transition), which indicates that the Eu^{3+} occupied the lattice sites without inversion symmetry in the $Ca_3Al_2O_6$ host.

3.4 TL and ESR

Un-irradiated $Ca_3Al_2O_6$:Eu^{3+} did not exhibit any TL glow peaks. Upon gamma irradiation (dose: 5 Gy), the phosphor exhibits three glow peaks around 195°C, 325°C and 390°C. Figure 5 shows the observed glow curve. The glow curves for the samples were obtained at a heating rate of 5°C/s.

Figure 6 shows the ESR spectrum at room temperature after gamma irradiation (dose:10 kGy) of $Ca_3Al_2O_6$:Eu^{3+} phosphor. Figure 6(a) corresponds to the spectrum recorded at a microwave power of 10 mW while the spectrum shown in Fig. 6(b) is recorded at a higher power value (32 mW) with increased receiver gain. At least three distinct centres appear to contribute to the observed spectrum. This inference is based on the observation of the spectra at different microwave powers and thermal-annealing experiments. It was possible to identify the three centres and one of the centres is labelled in Fig. 6(b). The ESR line labelled as centre I is due to a species characterized by a single broad line with an isotropic g-value equal to 2.0130 and 49 gauss linewidth. This line could be seen at a relatively high microwave power (above 30 mW) and is observed as a broad canopy overlaying the other relatively narrow multiple high intensity ESR lines belonging to centre II.

$Ca_3Al_2O_6$ is cubic, $a = 1.5263$ nm, space group *Pa3* and $Z = 24$ [42]. The structure consists of rings of six AlO_4 tetrahedra (Al_6O_{18}), eight to a unit cell, surrounding a hole of radius 0.147 nm, with Ca^{2+} ions holding the rings together. There are two types of Al cations and the environments of these ions are very similar. There are six types of

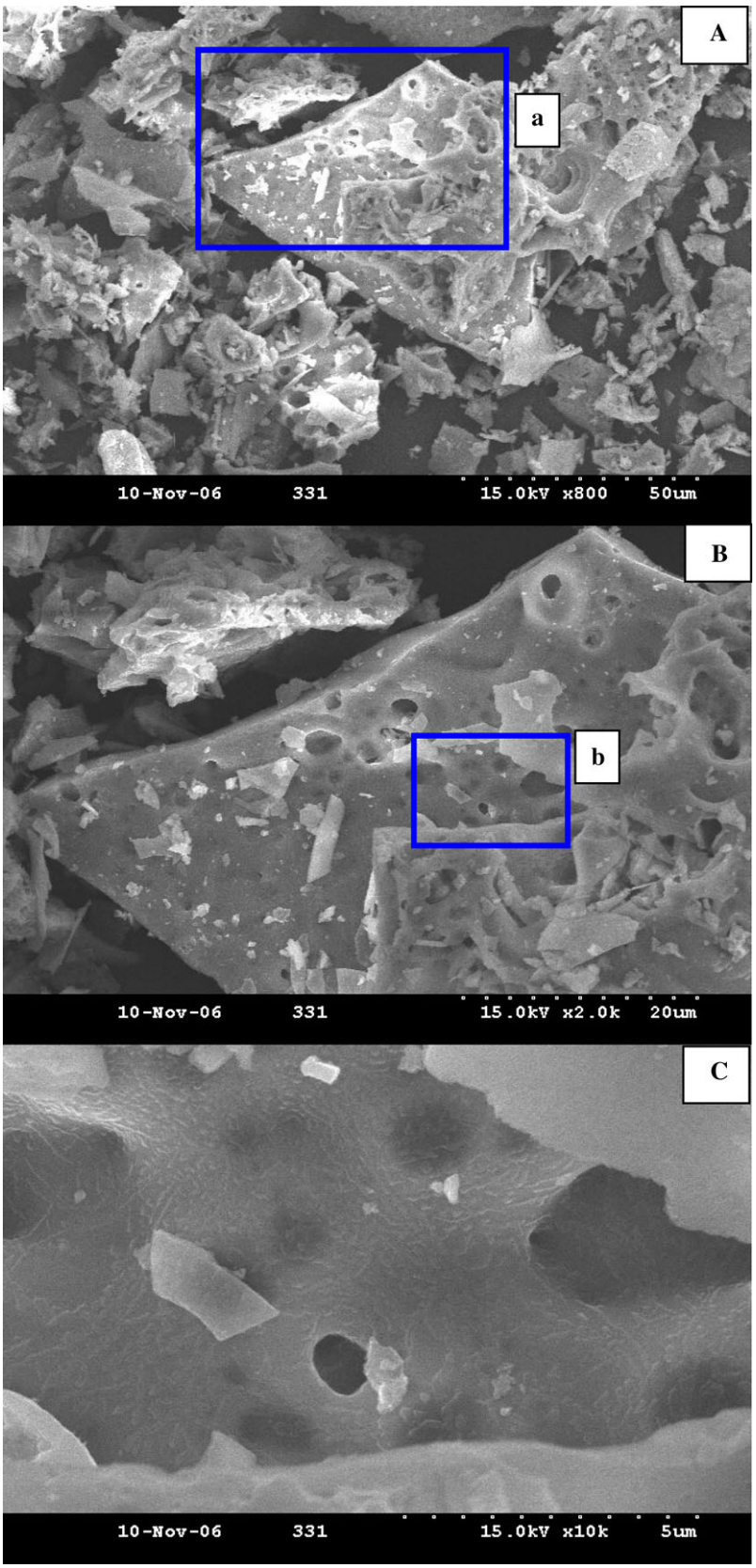

Fig. 2 SEM micrographs of the $Ca_3Al_2O_6$ powder

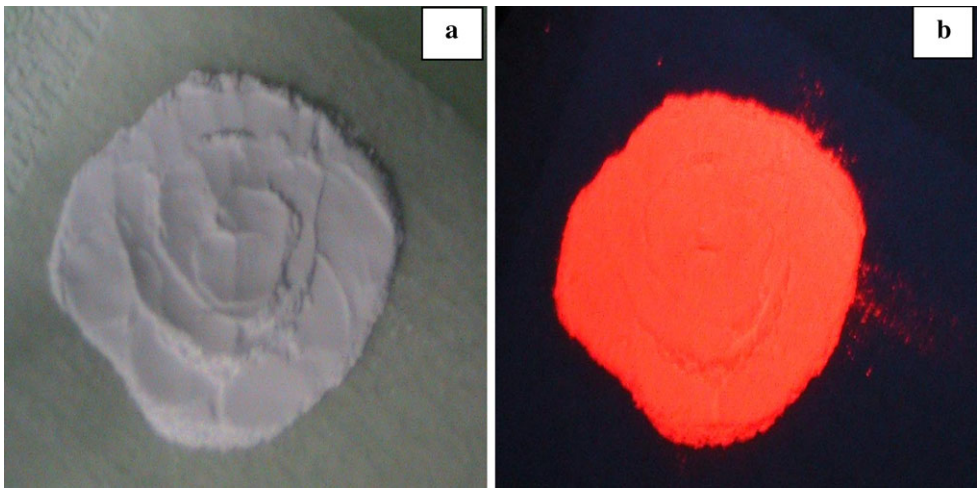

Fig. 3 Typical photographs of an as-prepared $Ca_3Al_2O_6$:Eu^{3+} phosphor sample under (**a**) room light (appearance: a white powder) and (**b**) 254 nm UV irradiation source (appearance: red emission of $^5D_0$–$^7F_2$ transition of Eu^{3+})

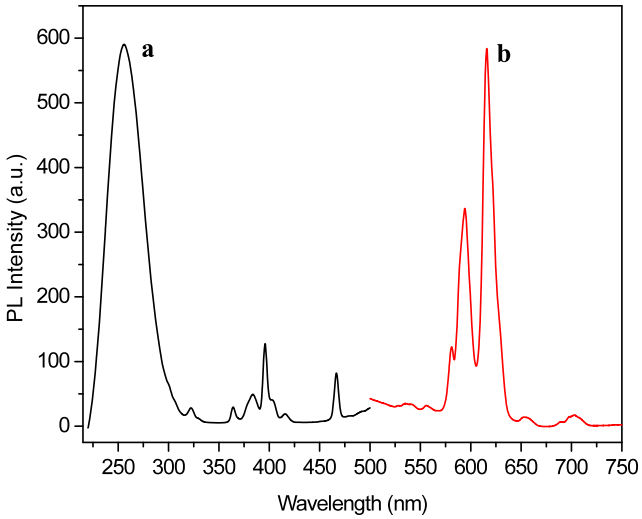

Fig. 4 Photoluminescence spectra of the: as-prepared $Ca_3Al_2O_6$:Eu^{3+} *a* excitation spectrum (λ_{em} = 616 nm) and *b* emission spectrum (λ_{ex} = 255 nm)

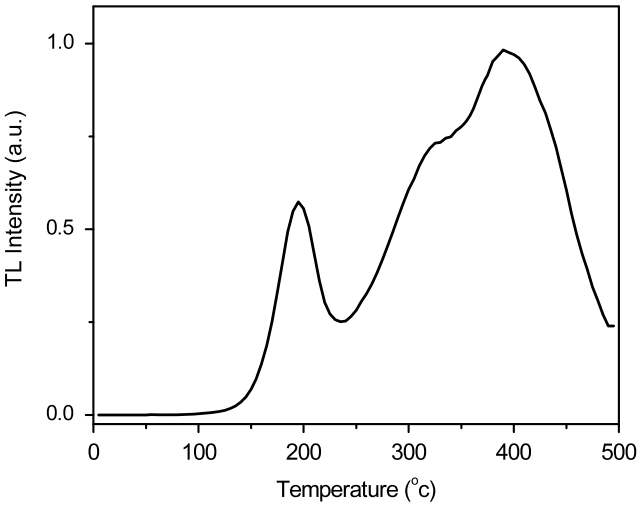

Fig. 5 TL glow curve of $Ca_3Al_2O_6$:Eu^{3+} phosphor (test gamma dose: 5 Gy)

Ca cations, three of which are six-coordinate: Ca(1), Ca(2) and Ca(3). The cations Ca(1) and Ca(2) have a compressed octahedral geometry and Ca(3) has a distorted trigonal prism geometry. The other Ca cations, Ca(4)–Ca(6), have higher coordination numbers and more distorted geometries. As there are divalent and trivalent ions occupying octahedral and tetrahedral lattice positions, respectively, antisite formation due to interchange of the cations on tetrahedral and octahedral lattice positions causes numerous trapping sites for the electron and hole on irradiation. Further, there can also be damage to the defect centres and impurities by irradiation which causes a change in their charge states [43]. Therefore, several defect centres are expected to be formed and the most probable centres which can be observed are the F^+ centres (an electron trapped at an anion vacancy) and O^- ions (a positive hole localized on an O^{2-} ion neighbouring a cation vacancy).

A large linewidth is exhibited by centre I which indicates unresolved hyperfine structure. The unresolved structure results from the interaction of the unpaired electron with nearby nuclear spins. Aluminium as well as calcium in $Ca_3Al_2O_6$ have isotopes with nuclear spins 5/2 (^{27}Al) and 7/2 (^{43}Ca). ^{27}Al is much more abundant (100%) than ^{43}Ca (0.135%) and its nuclear magnetic moment is higher (3.685) than that of ^{43}Ca (1.3173) [44]. It is likely, therefore, that the electronic spin will be interacting with aluminium ions. As mentioned above, cation disorder and non-stoichiometry of aluminates can provide a large number of lattice defects which may serve as trapping centres. In such a case, oxygen vacancies should lead to F^+ centres by trapping electrons. On the other hand, hole trapping at aluminium and calcium vacancies can lead to formation of O^- ions. The observed broad ESR line of centre I and the associated unresolved hyperfine structure indicate that the unpaired electron is delocalized and interacts with nearby nuclei. It has been men-

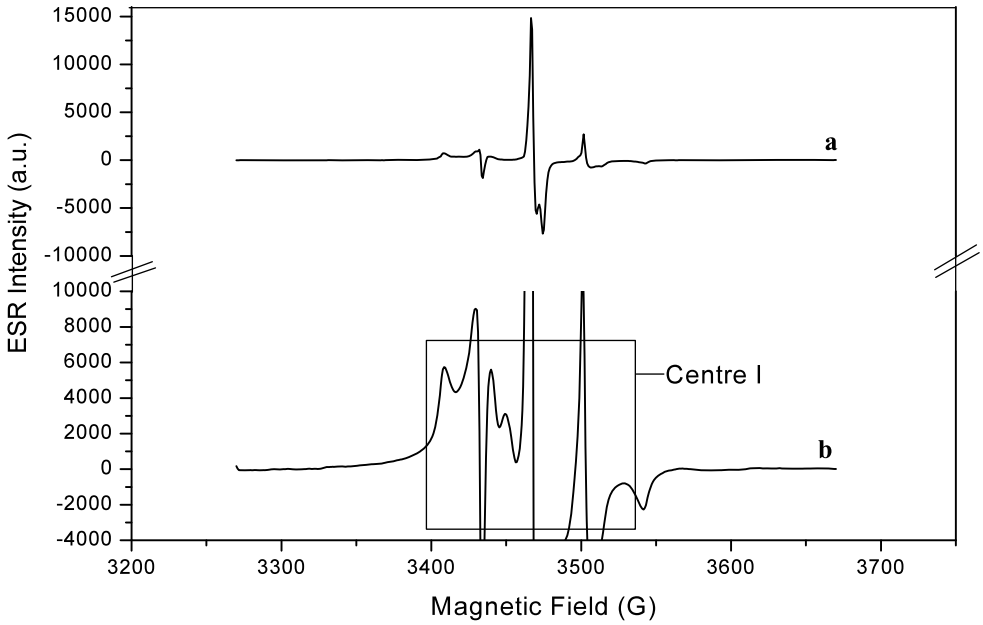

Fig. 6 Room-temperature ESR spectra of irradiated $Ca_3Al_2O_6:Eu^{3+}$ phosphor (gamma dose: 10 kGy). *a* spectrum recorded at 10 mW microwave power. *b* spectrum recorded at high microwave power (32 mW) and with increased receiver gain. The ESR lines observed in spectrum *a* are due to centre II. Centre II lines superpose centre I ESR line. Centre I line is observed as a broad canopy (49 gauss linewidth) overlapping the relatively narrow multiple ESR lines belonging to centre II. The box labelled as centre I in *b* indicates this broad line. Centre I is due to an O^- ion

tioned [45] that the charges in oxides must be trapped near double (or more) charged defects in order for the charge to be delocalized and thus allowing it to interact with surrounding nuclei. Hence centre I is tentatively assigned to an O^- ion stabilized by a nearby cation vacancy (a hole trapped in a Al^{3+}/Ca^{2+} ion vacancy). It may be mentioned that a similar centre in neutron irradiated $MgAl_2O_4$ has been assigned to an O^- ion [46].

A pulsed thermal-annealing method was used to measure the stability of centre I. After heating the sample up to a given temperature value where it is maintained for 3 minutes, it is cooled rapidly down to room temperature for ESR measurements. The thermal-annealing behaviour of centre I is shown in Fig. 7(a). It is observed that the centre becomes unstable around 130°C and decays in the temperature range 130–280°C. This decay appears to relate to the low temperature TL peak around 195°C. As there is overlap from ESR lines of other centres, the thermal-annealing result shown in Fig. 7 is only an approximate indicator of the decay behaviour of centre I.

Figure 8 shows the ESR spectrum from a sample which has been annealed at 220°C. In this annealed sample, centre I intensity has considerably reduced and the spectrum has been recorded specifically at low microwave power levels. At these low power levels, there is less interference from other ESR lines. The observed spectrum is characteristic of a species exhibiting an axially symmetric g-tensor with principal values $g_{\parallel} = 2.0030$ and $g_{\perp} = 2.0072$. The centre is found to exhibit hyperfine lines and the hyperfine splitting arises from an interaction between the electron spin on the centre and the nuclear spin of nearby two equivalent nuclei with spin $1/2$. The ESR spectrum consists of equally spaced hyperfine lines. The relative intensities of the lines [in Fig. 8,

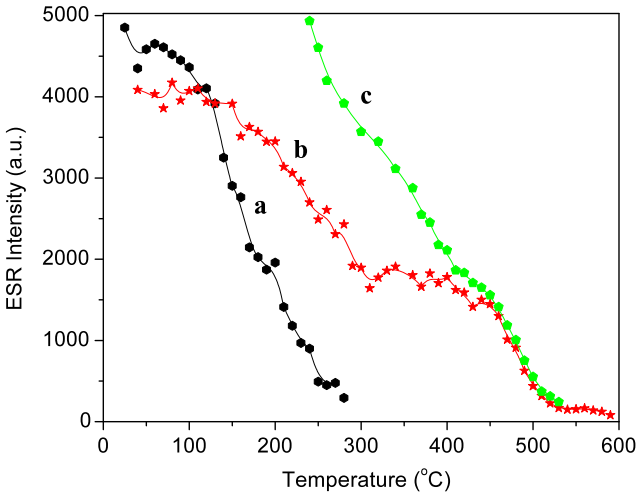

Fig. 7 Thermal-annealing behaviour of centres in $Ca_3Al_2O_6:Eu^{3+}$ phosphor. *a* corresponds to the annealing behaviour of centre I (O^-) whilst *b* and *c* refer to the annealing behaviour of centres II and III, respectively

(a) corresponds to perpendicular component hyperfine lines while (b) shows parallel component lines] are in reasonable agreement with those expected for an electron interacting equally with two nuclei of spin $1/2$, namely $1:2:1$. The principal values of the hyperfine tensor are $A_{\parallel} = 69$ gauss and $A_{\perp} = 35$ gauss.

In an earlier study of an oxide system, Yttria stabilized Zirconia (YSZ), i.e. ZrO_2:Y, a centre has been assigned to an F^+ centre (a singly charged oxygen vacancy with one remaining electron) by Costantini et al. [47]. An F^+ centre with zero angular momentum normally exhibits an isotropic *g*-value. The F^+ centre in YSZ, however, was characterized

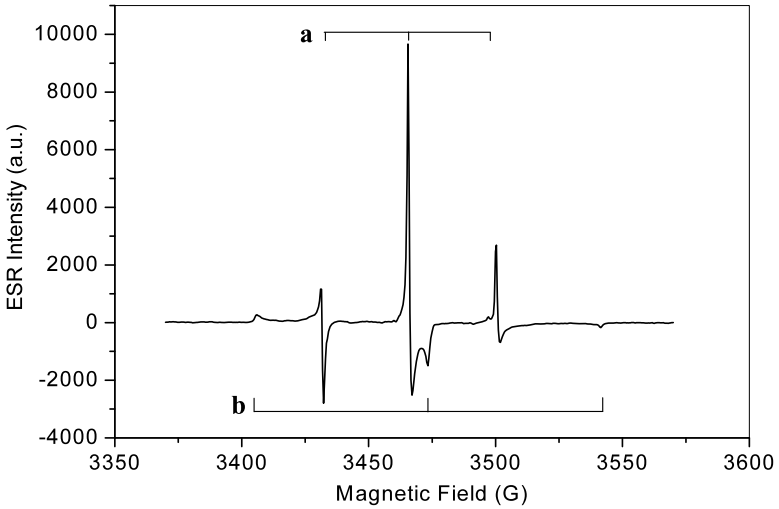

Fig. 8 ESR spectrum of irradiated and 220°C annealed $Ca_3Al_2O_6:Eu^{3+}$ phosphor (microwave power: 0.5 mW). The observed lines (centre II) are due to an F^+ centre. *a* refers to perpendicular component hyperfine lines and *b* corresponds to lines from parallel component

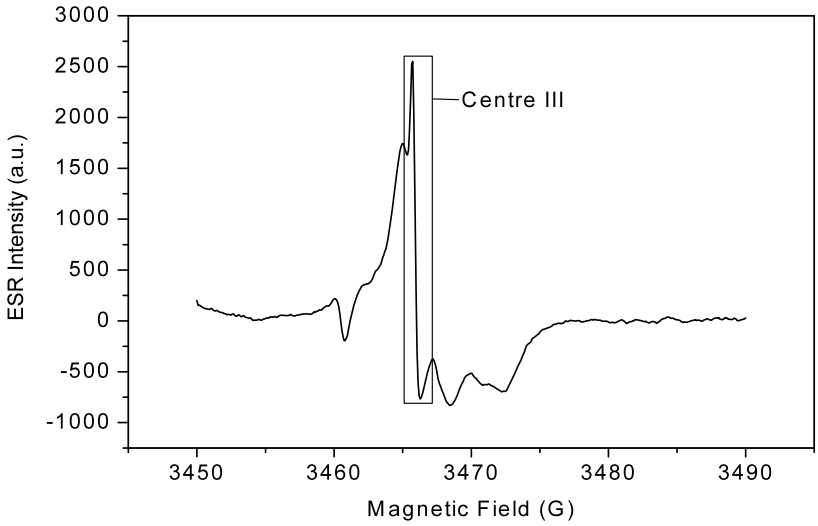

Fig. 9 Room-temperature ESR spectrum of irradiated $Ca_3Al_2O_6:Eu^{3+}$ phosphor recorded with lower modulation (0.5 gauss) and smaller scan range. Centre III line is assigned to an F^+ centre

by an axially symmetric *g*-tensor. In order to account for the axial nature of the *g*-tensor, Costantini et al. suggested that a symmetry breaking defect should be present at an anionic site near the F^+ centre. This anionic site defect assigned to a neutral F centre (oxygen vacancy with two electrons) appears to be consistent with the large density of oxygen vacancies present in the YSZ system. On the basis of results of Costantini et al., the defect centre II in $Ca_3Al_2O_6:Eu^{3+}$ is assigned to an F^+ centre. The axial nature of the *g*-tensor could result from an F centre present near the vicinity of centre II in a manner similar to YSZ. It is to be noted that $Sr_3Al_2O_6$ is isostructural with $Ca_3Al_2O_6$ and a structural study by Alonso et al. [48] have shown that a large number of oxygen vacancies are present in the lattice of $Sr_3Al_2O_6$ (48 per unit cell). These oxygen vacancies are also likely to be present in $Ca_3Al_2O_6:Eu^{3+}$ which can lead to the formation of F centres in close proximity to centre II.

Centre II's hyperfine structure indicates interaction of the unpaired electron with nearby nuclei of spin 1/2. ^{43}Ca and ^{27}Al have nuclear spins greater than 1/2 and it has not been possible to identify these nearby nuclei based on the present results. In an early ESR/ENDOR study of BeO single crystal, DuVarney et al. [49] observed that the unpaired electron trapped at an anion vacancy (F^+ centre) interacts with four nearest-neighbour (nn) Be nuclei. The hyperfine interaction observed in the present system is dipolar in nature with negligible isotropic component in contrast to the observations in BeO.

The thermal-annealing behaviour of centre II is shown in Fig. 7(b) and it is seen that the centre decays in two stages. The decay temperature range 150–300°C is associated with the TL peak at 195°C. Two stage decay of centre II shows that F^+ centre acts as a recombination centre when the hole from O^- ion (centre I) is released and recombines with the electron in F^+ centre. The second stage of decay is in the range 350–500°C and shows that centre II is also related to the high temperature TL peak at 390°C.

Centre III indicated in Fig. 9 is due to a centre characterized by a single ESR line with an isotropic g-value equal to 2.0073 and 1 gauss linewidth. As mentioned earlier, one of the probable centres which can be formed after irradiation in this phosphor is an F^+ centre (an electron trapped at an anion vacancy). Such a centre was first observed in neutron irradiated LiF [50]. In LiF, a single broad line (linewidth ∼100 gauss) with a g-factor equal to 2.008 was observed. F^+ centre inherently has a narrow linewidth of about 1 gauss (as observed in MgO system [51]). The experimentally observed linewidth is determined by the ions present in the system (whether they have nuclei with magnetic moment and their abundance) and also on the amount of delocalization of the unpaired electron which depends on the host lattice. In alkali halides, an unusually large linewidth is observed as the electron is delocalized and interacts with several alkali and halide ions from successive neighbouring shells. In KCl, the observed linewidth is around 20 gauss [52] and in LiCl it is 58 gauss [52]. In other systems like $HgI_2{\cdot}2HgS$ [53] and BaO [54], the linewidths are about 10 gauss and 3.5 gauss, respectively. In general, a variation in linewidth is observed. F^+ centres are characterized by a small g-shift, which may be positive or negative, a linewidth which depends on the host lattice and saturation properties characteristic of an in-homogeneously broadened ESR line. An anionic vacancy traps an electron during irradiation and such trapping is the basis for the formation of F^+ centres. Hyperfine interaction with the nearest-neighbour cations is the major contribution to the linewidth. Defect centre III formed in the present system is characterized by a small g-shift. The centre does not exhibit hyperfine structure. On the basis of these observations and considerations of the characteristic features of the defect centres likely to be formed in a system such as $Ca_3Al_2O_6$:Eu^{3+}, centre III is tentatively assigned to an F^+ centre.

Figure 7(c) shows the thermal-annealing behaviour of centre III. It is observed that the centre decays in two stages. The decay temperature range 260–400°C appears to correlate with the 325°C TL peak and the centre could be the recombination centre. The second stage of decay is in the temperature range 450–520°C and is not related to any of the TL peaks.

4 Conclusions

In summary, Eu^{3+} doped $Ca_3Al_2O_6$ powders were prepared in one step by the low temperature combustion synthesis. The major advantages of the combustion process are its simple, fast and energy saving procedures and its ability to produce direct crystallization of particles even at a low furnace temperature of 500°C. The PL spectra show the emission at 616 nm corresponding to the electric-dipole $^5D_0$–$^7F_2$ transition of Eu^{3+} in $Ca_3Al_2O_6$ due to the non-centrosymmetric nature of the Eu^{3+} site. Emission of Eu^{3+} is found to be particularly useful as a red emitting lamp phosphor as excitation wavelength overlaps with 254 nm of Hg emission. $Ca_3Al_2O_6$:Eu^{3+} phosphor exhibits three TL peaks at 195°C, 325°C and 390°C. ESR studies indicate three defect centres in the irradiated phosphor. These centres are tentatively assigned to an O^- ion and F^+ centres. O^- ion correlates with the 195°C TL peak. One of the F^+ centres appears to act as a recombination centre for the TL peak at 195°C and also is related to the TL peak at 390°C. A second F^+ centre appears to correlate with the 325°C TL peak.

Acknowledgements This paper is dedicated to the late Prof Dong-Kuk Kim, Department of Chemistry, Kyungpook National University, Daegu, South Korea. The author Vijay Singh expresses his thanks to the Hanse-Wissenschaftskolleg (Delmenhorst, Germany) for providing the research fellowship. T.K. Gundu Rao is grateful to FAPESP, Brazil for the research fellowship.

References

1. Y. Lin, Z. Zhang, Z. Tang, J. Zhang, Z. Zheng, X. Lu, Mater. Chem. Phys. **70**, 156 (2001)
2. D. Ravichandran, S.T. Johnson, S. Erdei, R. Roy, W.B. White, Displays **19**, 197 (1999)
3. A.J. Lenus, K.G. Rajan, M. Yousuf, D. Sornadurai, B. Purniah, Mater. Lett. **54**, 70 (2002)
4. S.R. Jansen, J.W. de Haan, L.J.M. van de Ven, R. Hanssen, H.T. Hintzen, R. Metselaar, Chem. Mater. **9**, 1516 (1997)
5. T. Peng, L. Huajun, H. Yang, C. Yan, Mater. Chem. Phys. **85**, 68 (2004)
6. S. Tanaka, I. Ozaki, T. Kunimoto, K. Ohmi, H. Kobayashi, J. Lumin. **87–89**, 1250 (2000)
7. H. Hosono, K. Yamazaki, Y. Abe, J. Am. Ceram. Soc. **68**, C304 (1985)
8. T. Murata, T. Tanoue, M. Iwasaki, K. Morinaga, T. Hase, J. Lumin. **114**, 207 (2005)
9. T. Aitasalo, J. Holsa, H. Jungner, M. Lastusaari, J. Niittykoski, M. Parkkinen, R. Valtonen, Opt. Mater. **26**, 113 (2004)
10. P.N.M. dos Anjos, E.C. Pereira, Y.G. Gobato, J. Alloys Compd. **391**, 277 (2005)
11. V. Singh, V. Natarajan, J.-J. Zhu, Opt. Mater. **30**, 468 (2007)
12. D. Haranath, P. Sharma, H. Chander, A. Ali, N. Bhalla, S.K. Halder, Mater. Chem. Phys. **101**, 163 (2007)
13. H. Kubo, H. Aizawa, T. Katsumata, S. Komuro, T. Morikawa, J. Cryst. Growth **275**, e1767 (2005)
14. K.L. Scrivener, J.-L. Cabiron, R. Letourneux, Cem. Concr. Res. **29**, 1215 (1999)
15. J.D. Birchall, A.J. Howard, K. Kendall, Nature (London) **289**, 388 (1981)
16. K. Kendall, J.D. Birchall, A.J. Howard, Philos. Trans. R. Soc. A **310**, 139 (1983)
17. A.A. Goktaas, M.C. Weinberg, J. Am. Ceram. Soc. **74**, 1066 (1991)
18. P. Mondal, J.W. Jeffery, Acta Crystallogr. B **31**, 689 (1975)
19. X. Yuan, Y.B. Xu, Y. He, Mater. Sci. Eng., A **447**, 142 (2007)
20. J.M.R. Mercury, A.H. De Aza, X. Turrillas, P. Pena, J. Solid State Chem. **177**, 866 (2004)
21. S.-J. Lee, E.A. Benson, W.M. Kriven, J. Am. Ceram. Soc. **82**, 2049 (1999)
22. J.H. Schulman, W.D. Compton, *Colour centres in Solids* (McMillan Company, New York, 1962)

23. B.V. Padlyak, Radiat. Eff. Defects Solids **158**, 411 (2003)
24. N.K. Porwal, R.M. Kadam, T.K. Seshagiri, V. Natarajan, A.R. Dhobale, A.G. Page, Radiat. Meas. **40**, 69 (2005)
25. T.K. Seshagiri, M. Mohapatra, T.K. Gundu Rao, R.M. Kadam, V. Natarajan, S.V. Godbole, J. Phys. Chem. Solids **70**, 1261 (2009)
26. M. Kumar, R.M. Kadam, T.K. Seshagiri, V. Natarajan, A.G. Page, J. Radioanal. Nucl. Chem. **262**, 633 (2004)
27. S.J. Dhoble, S.V. Moharil, T.K. Gundu Rao, J. Lumin. **93**, 43 (2001)
28. V. Singh, T.K.G. Rao, J.-J. Miao, J.-J. Zhu, Radiat. Eff. Defects Solids **160**, 265 (2005)
29. V. Singh, T.K.G. Rao, J.-J. Zhu, J. Solid State Chem. **179**, 2589 (2006)
30. V. Singh, T.K.G. Rao, J. Solid State Chem. **181**, 1387 (2008)
31. V. Singh, V.K. Rai, I. Ledoux-Rak, S. Watanabe, T.K.G. Rao, J.F.D. Chubaci, L. Badie, F. Pelle, S. Ivanova, J. Phys. D, Appl. Phys. **42**, 065104 (2009)
32. V. Singh, S. Watanabe, T.K.G. Rao, J.F.D. Chubaci, I. Ledoux-Rak, H.-Y. Kwak, Appl. Phys. B **98**, 165 (2010)
33. S.R. Jain, K.C. Adiga, V.R.P. Vernekar, Combust. Flame **40**, 71 (1981)
34. V. Singh, R.P.S. Chakradhar, J.L. Rao, I. Ledoux-Rak, H.-Y. Kwak, J. Mater. Sci. **46**, 1038 (2011)
35. B.S. Barros, P.S. Melo, R.H.G.A. Kiminami, A.C.F.M. Costa, G.F. de Sá, S. Alves Jr, J. Mater. Sci. **41**, 4744 (2006)
36. J.J. Kingsley, K.C. Patil, Mater. Lett. **6**, 427 (1988)
37. N.A. Dhas, K.C. Patil, J. Solid State Chem. **102**, 440 (1993)
38. S.S. Manoharan, N.R.S. Kumar, K.C. Patil, Mater. Res. Bull. **25**, 731 (1990)
39. J.J. Kingsley, K. Suresh, K.C. Patil, J. Solid State Chem. **88**, 435 (1990)
40. J. Williamson, E.P. Glasser, J. Appl. Chem. **12**, 535 (1962)
41. V.K. Singh, M.M. Ali, U.K. Mandal, J. Am. Ceram. Soc. **73**, 872 (1990)
42. P. Mondal, J.W. Jeffrey, Acta Crystallogr. Sect. B **31**, 689 (1975)
43. G.P. Summers, G.S. White, K.H. Lee, J.H. Crawford, Phys. Rev. B **21**, 2578 (1980)
44. R.C. Weast (ed.), *Handbook of Chemistry and Physics* (CRC, Cleveland, 1971)
45. N.Y. Konstantinov, L.V. Karaseva, V.V. Gromov, Dokl. Akad. Nauk SSSR **228**, 631 (1980)
46. V.T. Gritsyna, V.A. Kobyakov, Zh. Tekh. Fiz. **55**, 354 (1985) [Sov. Phys. Tech. Phys. **30**, 206 (1985)]
47. J.M. Costantini, F. Beuneu, D. Gourier, C. Trautmann, G. Calas, M. Toulemonde, J. Phys., Condens. Matter **16**, 3957 (2004)
48. J.A. Alonso, I. Rasines, J.L. Soubeyroux, Inorg. Chem. **29**, 4768 (1990)
49. R.C. DuVarney, A.K. Garrison, R.H. Thorland, Phys. Rev. **188**, 657 (1969)
50. C.A. Hutchison, Phys. Rev. **75**, 1769 (1949)
51. J.E. Wertz, P. Auzins, R.A. Weeks, R.H. Silsbee, Phys. Rev. **107**, 1535 (1957)
52. W.C. Holton, H. Blum, Phys. Rev. **125**, 89 (1962)
53. K. Takei, H. Hagiwara, H. Tanaka, Bull. Chem. Soc. Jpn. **50**, 1341 (1977)
54. A.J. Tench, R.L. Nelson, Proc. Phys. Soc. **92**, 1055 (1967)